

# Super-Quasi-Orthogonal Space–Time Trellis Codes for Four Transmit Antennas

Hamid Jafarkhani and Navid Hassanpour

**Abstract**—We introduce a new family of space–time trellis codes that extends the powerful characteristics of super-orthogonal space–time trellis codes to four transmit antennas. We consider a family of quasi-orthogonal space–time block codes as building blocks in our new trellis codes. These codes combine set partitioning and a super set of quasi-orthogonal space–time block codes in a systematic way to provide full diversity and improved coding gain. The result is a powerful code that provides full rate, full diversity, and high coding gain. It is also possible to maintain a tradeoff between coding gain and rate. Simulation results demonstrate the good performance of our new super-quasi-orthogonal space–time trellis codes.

**Index Terms**—Quasi-orthogonal designs, set partitioning, space–time codes, super-orthogonal codes, transmitter diversity, trellis codes.

## I. INTRODUCTION

SPACE–TIME trellis codes have been introduced in [1] to provide improved error performance for wireless systems using multiple transmit antennas. The authors have shown that such codes can provide full diversity gain, as well as additional signal-to-noise ratio (SNR) advantage that they call the coding gain. Code design rules for achieving full diversity for two transmit antennas are also provided. Using these design rules, examples of codes, for two transmit antennas, with full diversity, as well as some coding gain were constructed that are not necessarily optimal.

In [2], Alamouti introduced a simple code to provide full diversity for two transmit antennas. In [3], the scheme is generalized to an arbitrary number of antennas and is named space–time block coding. Also, the theory of orthogonal designs has been generalized in [3] to show when it is possible to achieve full diversity. Although a space–time block code provides full diversity and a very simple decoding scheme, despite the name, its main goal is not to provide additional coding gain [3], [4]. This is in contrast to space–time trellis codes that provide full diversity, as well as coding gain but at a cost of higher decoding complexity.

A new class of space–time codes called super-orthogonal space–time trellis codes (SOSTTCs) was introduced in [5]. A

Manuscript received November 25, 2003; revised July 1, 2003; accepted November 17, 2003. The editor coordinating the review of this paper and approving it for publication is F.-C. Zheng. The work of H. Jafarkhani was supported in part by the National Science Foundation (NSF) under NSF Career Award CCR-0238042.

H. Jafarkhani is with the Department of Electrical Engineering and Computer Science, University of California, Irvine, Irvine, CA 92697 USA (e-mail: hamidj@uci.edu).

N. Hassanpour is with the Department of Electrical Engineering, Stanford University, Stanford, CA 94305 USA (e-mail: navid@stanford.edu).

Digital Object Identifier 10.1109/TWC.2004.840247

similar independent work was done in [6]. These codes combine set partitioning and a super set of orthogonal space–time block codes in a systematic way to provide full diversity and improved coding gain over earlier space–time trellis code constructions. The super-orthogonal set is derived by a constellation rotation. While providing full-diversity and full-rate, the structure of the new codes allows an increase in the coding gain. One shortcoming of the orthogonal space–time block codes is the fact that full-rate codes do not exist for more than two transmit antennas [3]. To combat this problem, quasi-orthogonal space–time block codes (QOSTBCs) have been proposed in the literature [7], [8] that provide full rate. One can rotate some of the signals in a quasi-orthogonal space–time block code to derive a code that provides full-diversity and full-rate. Independent examples of such a rotation are given in [9]–[11]. The result is powerful codes with simple pairwise decoding strategies. Some related work in the literature can be found in [12]–[14]. In this paper, first, we study the conditions for which a rotated QOSTBC provides full diversity, and then we combine the constellation rotations of SOSTTCs with that of QOSTBCs to systematically design a new class of space–time codes that provide full-rate, full-diversity, and very high coding gains for four transmit antennas. We call codes derived from this new structure super-quasi-orthogonal space–time trellis codes. We also provide a class of non-full-rate codes to tradeoff rate with coding gain. Not only do we show how to design a space–time trellis code for a given rate and number of states, but also our general set partitioning results provide the maximum coding gain for the proposed structure.

In Section II, first we provide a parameterized class of quasi-orthogonal space–time block codes and study the conditions to provide full diversity. Then, we study the set partitioning using phase shift keyed (PSK) constellation symbols in Section III. We provide coding gain analysis in Section IV. Using the new parameterized class of space–time block codes and our set partitioning, we show how to design optimal super-quasi-orthogonal space–time trellis codes for four transmit antennas in Section V. Non-full-rate codes that provide a tradeoff between rate and coding gain are designed in Section VI. We present simulation results in Section VII and provide some concluding remarks in Section VIII.

## II. FULL-DIVERSITY QUASI-ORTHOGONAL SPACE–TIME BLOCK CODES

Consider a space–time code using the transmission matrix  $\mathcal{G}$ . Let us denote the difference of the transmission matrices for codewords  $c_1$  and  $c_2$  by  $D(c_1, c_2)$  and its Hermetian, complex

conjugate and transpose by  $D^H(c_1, c_2)$ . Following the definitions in [1], the diversity of such a code is defined by the minimum rank of the matrix  $D(c_1, c_2)$ . For the case of  $N$  transmit antennas and one receive antenna, the maximum diversity is  $N$ . When  $D(c_1, c_2)$  is full-rank for every pair of codewords, the code is a full-diversity code and the minimum of the determinant of the matrix  $A(c_1, c_2) = D^H(c_1, c_2)D(c_1, c_2)$  over all possible pairs of distinct codewords  $c_1$  and  $c_2$  corresponds to the coding gain. We define the coding gain distance (CGD) between codewords  $c_1$  and  $c_2$  as  $\text{CGD}(c_1, c_2) = d^2(c_1, c_2) = \det(A(c_1, c_2))$ , where  $\det(A)$  is the determinant of matrix  $A$ . In general, if we have a code with diversity less than  $N$ , the distance can be defined as the harmonic mean of the nonzero eigenvalues of  $A(c_1, c_2)$ .

Full-rate orthogonal designs with complex elements in its transmission matrix are impossible for more than two transmit antennas [3]. The only example of a full-rate full-diversity complex space-time block code using orthogonal designs is the Alamouti scheme [2], which is defined by the following transmission matrix:

$$\mathcal{G}_{12} = \begin{pmatrix} x_1 & x_2 \\ -x_2^* & x_1^* \end{pmatrix}. \quad (1)$$

Here, we use the subscript 12 to represent the indeterminate variables  $x_1$  and  $x_2$  in the transmission matrix. Now, let us consider the following QOSTBC [7]:

$$\mathcal{G} = \begin{pmatrix} \mathcal{G}_{12} & \mathcal{G}_{34} \\ -\mathcal{G}_{34}^* & \mathcal{G}_{12}^* \end{pmatrix} = \begin{pmatrix} x_1 & x_2 & x_3 & x_4 \\ -x_2^* & x_1^* & -x_4^* & x_3^* \\ -x_3^* & -x_4^* & x_1^* & x_2^* \\ x_4 & -x_3 & -x_2 & x_1 \end{pmatrix} \quad (2)$$

where a matrix  $\mathcal{G}^*$  is the complex conjugate of  $\mathcal{G}$ . It has been shown in [7] that this is a full-rate code and symbols can be decoded in pairs. There are other examples in [7] with the same properties. Also, a similar quasi-orthogonal code is proposed in [8]

$$\mathcal{G} = \begin{pmatrix} \mathcal{G}_{12} & \mathcal{G}_{34} \\ \mathcal{G}_{34} & \mathcal{G}_{12} \end{pmatrix}. \quad (3)$$

It is easy to see that the minimum rank of the difference matrix  $D(c_1, c_2)$  is 2. Therefore, for  $M$  receive antennas, a diversity of  $2M$  is achieved, while the rate of the code is one. Note that it has been proved in [3] that the maximum diversity of  $4M$  for a rate one complex orthogonal code is impossible in this case if all signals are chosen from the same constellation. The maximum-likelihood decision metric can be calculated as the

sum of two terms such that one can decode pairs of symbols independently [7]. For  $x_3$  and  $x_4$  from the original constellation, let us denote  $\tilde{x}_3$  and  $\tilde{x}_4$  as the rotated symbols (with respect to  $x_3$  and  $x_4$ ). One can show that it is possible to provide full-diversity QOSTBCs by replacing  $(x_3, x_4)$  with  $(\tilde{x}_3, \tilde{x}_4)$ . Independent examples of such full-diversity QOSTBCs are provided in [9]–[11]. The resulting code is very powerful since it provides full diversity, full rate, and simple (pairwise) decoding with good performance.

In what follows, first, we derive the general conditions to achieve full diversity for this code.

*Lemma 2.1:* Consider two possible codewords  $c_1 = (x_1, x_2, \tilde{x}_3, \tilde{x}_4)$  and  $c_2 = (y_1, y_2, \tilde{y}_3, \tilde{y}_4)$ . Then

$$\text{CGD}(c_1, c_2) = \left( \sum_{i=1}^2 |(x_i - y_i) + (\tilde{x}_{2+i} - \tilde{y}_{2+i})|^2 \right)^2 \times \left( \sum_{i=1}^2 |(x_i - y_i) - (\tilde{x}_{2+i} - \tilde{y}_{2+i})|^2 \right)^2 \quad (4)$$

for the QOSTBC in (3). The same formula holds for the code in (2) if we arrange the codewords as  $c_1 = (x_1, x_2, -\tilde{x}_4, \tilde{x}_3)$  and  $c_2 = (y_1, y_2, -\tilde{y}_4, \tilde{y}_3)$ .

*Proof:* For the code in (3), the proof is given in [10]. For the code in (2), we have (5) at the bottom of the page. Then, one can show

$$\det(\mathcal{G}^H \mathcal{G}) = (|x_1 + x_4|^2 + |x_2 - x_3|^2)^2 (|x_1 - x_4|^2 + |x_2 + x_3|^2)^2. \quad (6)$$

Now, replacing  $x_1$  with  $x_1 - y_1$ ,  $x_2$  with  $x_2 - y_2$ ,  $x_3$  with  $-(\tilde{x}_4 - \tilde{y}_4)$ , and  $\tilde{x}_4$  with  $\tilde{x}_3 - \tilde{y}_3$  results in (4).  $\square$

Note that since (4) unifies the coding gain formula for both of the codes in (2) and (3), the two codes would have similar properties. In what follows, with a slight abuse of the notation, we use  $c = (x_1, x_2, \tilde{x}_3, \tilde{x}_4)$  along with (4) for both codes. However, one should keep in mind that for the code in (2), the codeword is in fact  $c = (x_1, x_2, -\tilde{x}_4, \tilde{x}_3)$ . This one-to-one replacement is the only difference between the two codes as far as our results and new codes are concerned.

*Lemma 2.2:* The quasi-orthogonal code provides full diversity if and only if the rotated constellation is such that  $x_i - y_i = \tilde{x}_{2+i} - \tilde{y}_{2+i}$ ,  $i = 1, 2$  is impossible for distinct codewords.

*Proof:* Full diversity is achieved if and only if the CGD in (4) is not zero. If the CGD becomes zero, then at least one of the two factors in (4) should be zero. To find the minimum CGD, we consider all possible values of  $x_i$ ,  $y_i$ ,  $\tilde{x}_{2+i}$ , and  $\tilde{y}_{2+i}$ ,  $i = 1, 2$ . If there is a set of values such that

$$\mathcal{G}^H \mathcal{G} = \begin{pmatrix} \sum_{i=1}^4 |x_i|^2 & 0 & 0 & 2\text{Re}(x_1^* x_4 - x_2 x_3^*) \\ 0 & \sum_{i=1}^4 |x_i|^2 & 2\text{Re}(x_2 x_3^* - x_1^* x_4) & 0 \\ 0 & 2\text{Re}(x_2 x_3^* - x_1^* x_4) & \sum_{i=1}^4 |x_i|^2 & 0 \\ 2\text{Re}(x_1^* x_4 - x_2 x_3^*) & 0 & 0 & \sum_{i=1}^4 |x_i|^2 \end{pmatrix} \quad (5)$$

$\sum_{i=1}^2 |(x_i - y_i) + (\tilde{x}_{2+i} - \tilde{y}_{2+i})|^2 = 0$ , by switching  $\tilde{x}_{2+i}$  with  $\tilde{y}_{2+i}$ , we have  $\sum_{i=1}^2 |(x_i - y_i) - (\tilde{x}_{2+i} - \tilde{y}_{2+i})|^2 = 0$  as well. Therefore, without loss of generality, we only need to consider the case that the second factor becomes zero. All terms of the sum are nonnegative. Therefore, the sum is zero only when all of its terms are zero and *vice versa*. If none of the two pairs of signals results in  $x_i - y_i = \tilde{x}_{2+i} - \tilde{y}_{2+i}$ , we conclude that the second, and consequently, the first factor is not equal to zero. Also, if the first and the second factors are not zero,  $x_i - y_i \neq \tilde{x}_{2+i} - \tilde{y}_{2+i}$  for any two distinct pairs of signals.  $\square$

We consider the validity of this inequality in the special case of  $L$ -PSK constellations and demonstrate the necessary conditions to obtain full diversity in this case. We consider  $L$ -PSK constellations, where the signals can be represented as  $e^{j2\pi l/L}$ ,  $l = 0, 1, \dots, L-1$ . We study the case of even and odd values of  $L$  separately. First, we consider the case of even  $L$ .

*Theorem 2.1:* If we pick  $x_i, i = 1, 2$  signals from an  $L$ -PSK constellation with even  $L$  and  $\tilde{x}_{2+i}$  signals from the rotated constellation, the resulting QOSTBC provides full diversity.

*Proof:* First, we show that if  $x_i$  belongs to an  $L$ -PSK constellation point and  $L$  is even,  $-x_i$  is also a point of the constellation. For  $L$ -PSK constellation points, we have  $x_i = e^{j2\pi l/L}$  for some value of  $l = 0, 1, \dots, L-1$ . Calculating  $-x_i = e^{j\pi} x_i = e^{j2\pi(l+L/2)/L} = e^{j2\pi l'/L}$  shows that  $-x_i$  belongs to the same  $L$ -PSK constellation.

To prove the theorem, using Lemma 2.2, we need to show that it is impossible for any values of  $S_i, S_j$  from the original constellation and  $T_k, T_l$  from the rotated constellation to have  $S_i + S_j = T_k + T_l \neq 0$ . We know that  $S_i + S_j \neq 0$  is a vector which is placed on the bisector of  $S_i$  and  $S_j$ . Suppose that  $T_k$  and  $T_l$  from the rotated constellation can have a sum  $T_k + T_l$  equal to  $S_i + S_j$ . Then, we assume

$$\begin{aligned} \angle(S_i, S_i + S_j) &= \angle(S_j, S_i + S_j) = \alpha \\ \angle(T_k, T_k + T_l) &= \angle(T_l, T_k + T_l) = \beta. \end{aligned} \quad (7)$$

Therefore,  $|T_k + T_l|^2 = |S_i + S_j|^2$  results in  $|T_k|^2 + |T_l|^2 + 2T_k \cdot T_l = |S_i|^2 + |S_j|^2 + 2S_i \cdot S_j$ , or equivalently,  $|T_k||T_l| \cos 2\beta = |S_i||S_j| \cos 2\alpha$ . This results in one of the following two equalities

$$2\alpha = 2\beta \text{ or} \quad (8)$$

$$2\alpha = 2\pi - 2\beta. \quad (9)$$

Neither of these equations can be true because  $\alpha = \beta$  results in  $S_i = T_l$  and  $S_j = T_k$  that is impossible and  $\alpha = \pi - \beta$  results in another set of impossible equations  $S_i = -T_k$  and  $S_j = -T_l$ .  $\square$

For odd  $L$ , we prove the following theorem.

*Theorem 2.2:* For an  $L$ -PSK constellation,  $L$  odd, if the rotation  $\phi = \pi/L$ , the code is not full diversity. Otherwise, the code provides full diversity.

*Proof:* For  $L$ -PSK constellation points, we have  $x_i = e^{j2\pi l/L}$  for some value of  $l = 0, 1, \dots, L-1$ . Then,  $-x_i = e^{j\pi} x_i = e^{j2\pi(l+L/2)/L}$ . Since  $L$  is odd, there is an  $m$  such that  $L = 2m + 1$ , which results in  $-x_i = e^{j2\pi l'/L} e^{j\pi/L}$ . Therefore, if  $x_i$  belongs to an  $L$ -PSK constellation with odd  $L$ , then  $-x_i$  is in the constellation resulting from the rotation of the initial  $L$ -PSK constellation by  $\phi = \pi/L$ . In other words,

every point of the initial  $L$ -PSK constellation is an edge of a diameter of the circle that passes through all  $L$ -PSK points and if it is replaced by the other edge of the diameter, the result is another  $L$ -PSK constellation rotated by  $\phi = \pi/L$ .

Using the above result, for any pair  $S_i$  and  $S_j$ , one can write  $S_i - S_j = T_k - T_l$ , where  $T_k = -S_i$  and  $T_l = -S_j$  are from the rotated constellation. Therefore, for every difference between two signals of the original  $L$ -PSK constellation, there is an equal difference term between two signals from the rotated constellation. If these four signals are part of the two codewords, the resulting coding gain is zero which shows the code does not provide full diversity. For other rotations, the proof of full diversity is similar to that of Theorem 2.1.  $\square$

Theorems 2.1 and 2.2 show that the proposed rotated QOSTBC provides full diversity and full rate unless we use an  $L$ -PSK constellation with odd  $L$  and a rotation  $\phi = \pi/L$ . In [10], the authors provide a list of rotations that achieve the maximum coding gains for different examples of popular constellations.

### III. SET PARTITIONING

To design a super quasi-orthogonal space-time trellis code, we follow the general method in [5]. First, we need to do *set partitioning*. The number of signals to be partitioned varies with the fourth power of the constellation cardinality, e.g.,  $8^4 = 4096$  for 8-PSK. We provide a complete study of set partitioning for binary phase-shift keying (BPSK) and quadrature phase-shift keying (QPSK) for four transmit antennas and present a general algorithm for obtaining the set partitioning of an arbitrary  $L$ -PSK from the set partitioning of an  $L/2$ -PSK ( $L$  is even). Our set partitioning is similar to the schemes proposed for multiple trellis coded modulation (MTCM) in [15] although the case of four components is not considered there.

In this section, we assume that  $x_1, x_2, x_3$ , and  $x_4$  are symbols from an  $L$ -PSK constellation (even  $L$ ) and  $x_3$  and  $x_4$  are rotated by  $\pi/L$  to derive  $\tilde{x}_3$  and  $\tilde{x}_4$ . The resulting quasi-orthogonal code is full diversity due to Theorem 2.1. Note that rotating  $(x_1, x_2)$  instead of  $(x_3, x_4)$  results in similar properties and Theorem 2.1 is still valid. The index assignment for an  $L$ -PSK constellation is such that an index  $l$  represents a symbol  $e^{j2\pi l/L}$ . We provide the indices for  $x_1, x_2, x_3$ , and  $x_4$  in all tables and figures. The resulting symbols  $\tilde{x}_3$  and  $\tilde{x}_4$  are derived by applying the corresponding rotations. Fig. 1 shows an example of set partitioning for BPSK. In Fig. 1, the rotation is  $\pi/2$  and 0, 1 represent 1,  $-1$ , respectively. Note that  $\pi/2$  is the optimum rotation in that it provides the maximum coding gain for a quasi-orthogonal space-time block code using BPSK. Also, clearly 0, 1, respectively, represent  $j, -j$  after applying the rotation for the third or fourth symbols. Table I presents a similar set partitioning for QPSK. Similarly, we have picked a rotation of  $\pi/4$  for QPSK since it is the optimum rotation, i.e., it provides the maximum coding gain for a quasi-orthogonal space-time block code. The resulting constellation is very similar to a  $\pi/4$ -QPSK constellation [16].

One can find the best set partitioning for a given constellation by an exhaustive search. The minimum CGD at each layer of such an optimal set partitioning is maximum among those of

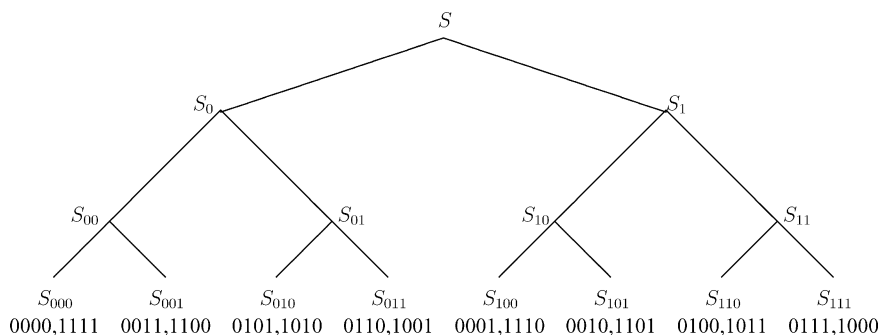


Fig. 1. Set partitioning for BPSK.

TABLE I  
SET PARTITIONING FOR QPSK

S															
S <sub>0</sub>								S <sub>1</sub>							
S <sub>00</sub>				S <sub>01</sub>				S <sub>10</sub>				S <sub>11</sub>			
S <sub>0000</sub>	S <sub>0001</sub>	S <sub>0010</sub>	S <sub>0011</sub>	S <sub>0100</sub>	S <sub>0101</sub>	S <sub>0110</sub>	S <sub>0111</sub>	S <sub>1000</sub>	S <sub>1001</sub>	S <sub>1010</sub>	S <sub>1011</sub>	S <sub>1100</sub>	S <sub>1101</sub>	S <sub>1110</sub>	S <sub>1111</sub>
0000	0020	1100	1120	0101	0121	1001	1021	0001	0021	1101	1121	0100	0120	1000	1020
2222	2202	3322	3302	2323	2303	3223	3203	2223	2203	3323	3303	2322	2302	3222	3202
2200	0002	3300	1102	2301	0103	3201	1003	2201	0003	3301	1103	2300	0102	3200	1002
0022	2220	1122	3320	0123	2321	1023	3221	0023	2221	1123	3321	0122	2320	1022	3220
****	****	****	****	****	****	****	****	****	****	****	****	****	****	****	****
2020	0200	3120	1300	0321	2101	3021	1201	2021	0201	3121	1301	0320	2100	3020	1200
0202	2022	1302	3122	2103	0323	1203	3023	0203	2023	1303	3123	2102	0322	1202	3022
2002	2000	3102	3100	0303	0301	3003	3001	2003	2001	3103	3101	0302	0300	3002	3000
0220	0222	1320	1322	2121	2123	1221	1223	0221	0223	1321	1323	2120	2122	1220	1222
****	****	****	****	****	****	****	****	****	****	****	****	****	****	****	****
1111	1131	0011	0031	1010	1012	0110	0112	1110	1130	0010	0030	1011	1013	0111	0113
3333	3313	2233	2213	3232	3230	2332	2330	3332	3312	2232	2212	3233	3231	2333	2331
3311	1113	2211	0013	3210	1030	2310	0130	3310	1112	2210	0012	3211	1031	2311	0131
1133	3331	0033	2231	1032	3212	0132	2312	1132	3330	0032	2230	1033	3213	0133	2313
****	****	****	****	****	****	****	****	****	****	****	****	****	****	****	****
3131	1311	2031	0211	3012	1210	0312	2110	3130	1310	2030	0210	3013	1211	0313	2111
1313	3133	0213	2033	1230	3032	2130	0332	1312	3132	0212	2032	1231	3033	2131	0333
3113	3111	2013	2011	3030	3010	0330	0310	3112	3110	2012	2010	3031	3011	0331	0311
1331	1333	0231	0233	1212	1232	2112	2132	1330	1332	0230	0232	1213	1233	2113	2133

all possible set partitioning trees. Such an exhaustive search may be time consuming for large constellations. However, since it is done once and only to design the codes, the high complexity may be acceptable. In this paper, we present an inductive algorithm for the set partitioning of  $L$ -PSK using the set partitioning of  $L/2$ -PSK when  $L$  is even and the rotation is  $\phi = \pi/L$ . Our algorithm reduces the complexity of the exhaustive search dramatically. The number of quadruplets for  $L$ -PSK is 16 times that of  $L/2$ -PSK. Therefore, when we go from  $L/2$ -PSK to  $L$ -PSK, the same level of the tree from the top includes 16 times more members and the tree includes more layers of subsets. The way we handle this 16-fold increase in the number of elements in each set is as follows. Note that the index  $l = 2l'$  in the  $L$ -PSK and the index  $l'$  in the  $L/2$ -PSK represent the same symbol. To increase the number of elements in a set by a factor of 16, we add all  $2^4 = 16$  combinations of 0 and  $L/2$  to the elements of the original set in a quadruplet, as in Fig. 2. It gives us eight new subsets for  $L$ -PSK under each subset of  $L/2$ -PSK. The three binary indices after letter  $T$  in Fig. 2 are added to the index of the

subset in the  $L/2$ -PSK set partitioning. Then, one may need to move some of the new subsets to maximize CGD at each level of set partitioning. For example, we consider the derivation of the set partitioning for QPSK from that of BPSK. In this case,  $L = 4$  and a set partitioning for QPSK is derived by adding the new subsets using Fig. 2. To maximize CGD, we need to switch subsets  $S_{00001}$  and  $S_{00010}$  (derived from Fig. 2), as we have done in Table I. Similarly, we have switched  $S_{00101}$  with  $S_{00110}$ ,  $S_{01001}$  with  $S_{01010}$ , and  $S_{01101}$  with  $S_{01110}$  to increase the CGD. Corresponding subsets rooted in set  $S_1$  have been switched to achieve the set partitioning in Table I. Fig. 3 demonstrates the details of one example of such a switching. Using the splitting in Fig. 2 for  $S_{00}$  results in the partitioning in Fig. 3(a). As can be seen from this figure, the minimum CGD for subsets  $S_{00000}$ ,  $S_{00001}$ ,  $S_{00010}$ , and  $S_{00011}$  is 256. By switching  $S_{00001}$  and  $S_{00010}$  (also  $S_{00101}$  with  $S_{00110}$ ), as in Fig. 3(b), the minimum CGD for subsets  $S_{00000}$ ,  $S_{00001}$ ,  $S_{00010}$ , and  $S_{00011}$  is 1024 which is higher than 256.

We study the details of CGD analysis for different subsets in the next section.

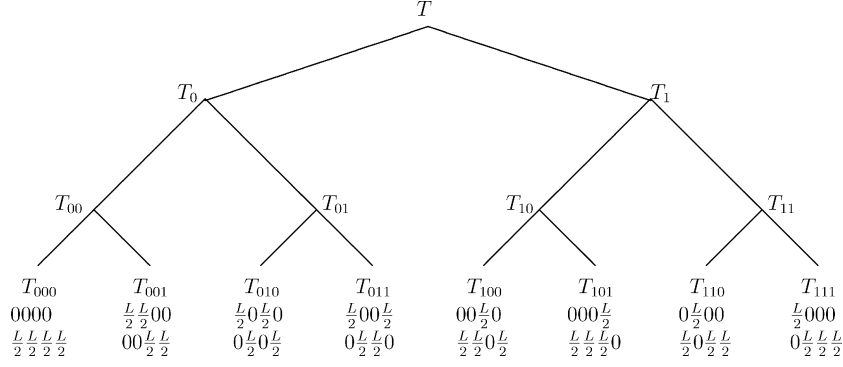
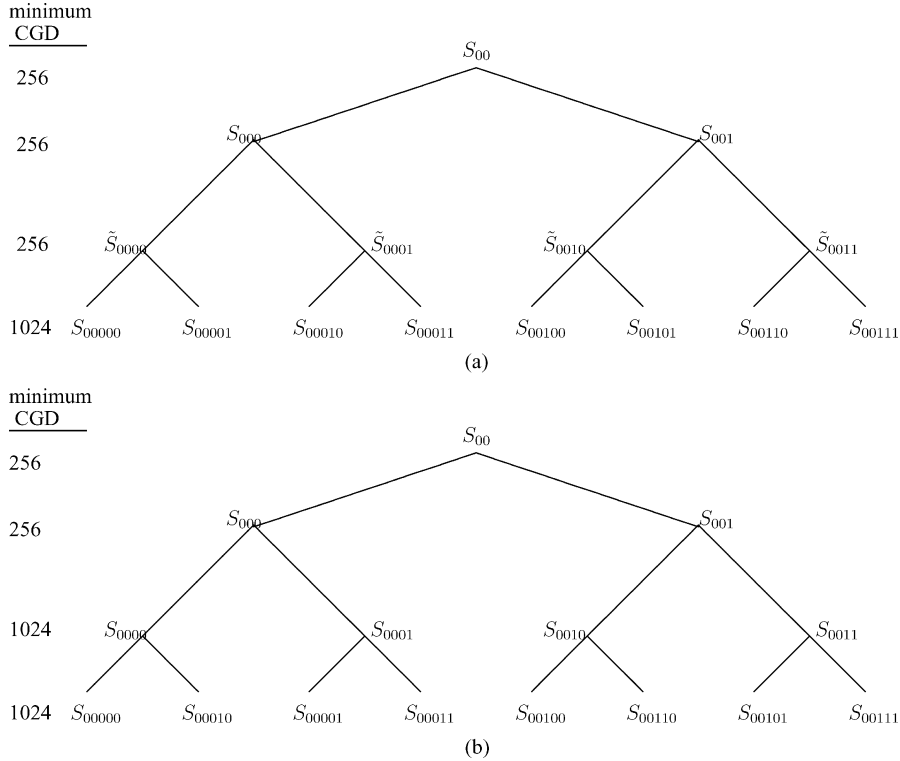
Fig. 2. New subsets created by all combinations of 0 and  $L/2$ .

Fig. 3. Subtree of set partitioning for four transmit antennas (QPSK). (a) Based on Fig. 2. (b) After switching some of the subsets to achieve higher CGD.

#### IV. CGD ANALYSIS

In this section, we study how to calculate the CGD of each subset in our set partitioning. To calculate the CGD of different subsets one needs to calculate the CGD between each possible codeword pair in the set and find the minimum CGD. There are two approaches to calculate the CGD between a pair of codewords. The first approach is to calculate the CGD by computer simulation. The second approach is to calculate it analytically using closed-form formulas. In this section, we consider the second approach since the first approach is straightforward. Let us consider the following pair of four  $L$ -PSK signals as codewords:

$$\begin{aligned} x_1 &= e^{j\phi_1} & x_2 &= e^{j\phi_2} & x_3 &= e^{j\phi_3} & x_4 &= e^{j\phi_4} \\ y_1 &= e^{j\tilde{\phi}_1} & y_2 &= e^{j\tilde{\phi}_2} & y_3 &= e^{j\tilde{\phi}_3} & y_4 &= e^{j\tilde{\phi}_4}. \end{aligned} \quad (10)$$

We also define  $\Delta_i = \tilde{\phi}_i - \phi_i$  and  $x_3$  and  $x_4$  are multiplied by a phase shift  $e^{j\phi}$ ,  $\phi = \pi/L$  to generate  $\tilde{x}_3$  and  $\tilde{x}_4$ . In other words,  $\tilde{x}_3 = e^{j\phi} e^{j\phi_3}$ ,  $\tilde{x}_4 = e^{j\phi} e^{j\phi_4}$ ,  $\tilde{y}_3 = e^{j\phi} e^{j\tilde{\phi}_3}$ , and  $\tilde{y}_4 = e^{j\phi} e^{j\tilde{\phi}_4}$ . Therefore, we can write the difference matrix  $D(c_1, c_2)$  in terms of these new parameters, as shown in (11) at the bottom of the next page. As it is evident from (5) and the corresponding formula for the code in (3), the CGD, which is  $\det(D^H(c_1, c_2)D(c_1, c_2))$  only depends on  $\Delta_1, \Delta_2, \Delta_3, \Delta_4, \phi_3 - \phi_1, \phi_4 - \phi_2$  (or  $\phi_4 - \phi_1, \phi_3 - \phi_2$  instead of  $\phi_3 - \phi_1, \phi_4 - \phi_2$ ), and not the  $\phi_i$ 's themselves.

One of the important factors in calculating the CGD is the number of zeros that we have in the error matrix  $D(c_1, c_2)$ . The number of zeros in the matrix is directly related to the number of symbols that are the same in  $c_1$  and  $c_2$ . Since we have a quadruplet to work with, in general, there are four cases.

Case 1) Two codewords  $c_1$  and  $c_2$  differ in only one symbol for example quadruplets 0000 and 1000.

Case 2) Two codewords  $c_1$  and  $c_2$  differ in two symbols. This case is divided into two categories.

- a) When the different symbols belong to constellations with different rotations, for example, quadruplets 0000 and 1001.
- b) When the different symbols belong to constellations with the same rotations, for example, quadruplets 0000 and 1100.

Case 3) Two codewords  $c_1$  and  $c_2$  differ in three symbols. As we will show later, the CGD is never dominated by this case. As an example, quadruplets 0000 and 0111 differ in three symbols.

Case 4) Two codewords  $c_1$  and  $c_2$  differ in four symbols for example quadruplets 0000 and 1111.

The CGD of different subsets is dominated by different cases. To see how different cases dominate the calculation of the CGD, we consider different layers of set partitioning in Fig. 1. The CGD of subset  $S$  in Fig. 1 is dominated by Case 1). The CGD of subset  $S_0$  is dominated by Case 2a). The CGD of subset  $S_{00}$  is dominated by Case 2b). The CGD of subset  $S_{000}$  is dominated by Case 4). Note that the structure of our set partitioning is such that the CGD is never dominated by Case 3).

In what follows, we calculate the CGD of different cases separately. We consider an  $L$ -PSK constellation and  $\phi = \pi/L$  rotation for the third and fourth symbols. Note that similar results are valid if we rotate the first and second symbols instead of the third and fourth symbols.

#### A. Only One Difference

If there is only one difference between the symbols of  $c_1$  and  $c_2$ , then assuming a phase difference of  $\Delta$  between the different symbols, the CGD can be calculated using (11) as follows:

$$\text{CGD} = |1 - e^{j\Delta}|^8. \quad (12)$$

Using (12) for QPSK, if  $\Delta = \pi/2$ , for example quadruplets 1000 and 1001, then  $\text{CGD} = 16$ . On the other hand,  $\Delta = \pi$ , for example, quadruplets 3001 and 1001, results in  $\text{CGD} = 256$ . Note that the third and fourth symbols are rotated by  $\phi = \pi/4$  for QPSK.

#### B. Two Differences

Two codewords  $c_1$  and  $c_2$  can differ in two positions in different ways. In our set partitioning, the magnitude of the phase difference between the two pairs of the symbols that differ is the same, for example,  $\Delta = |\Delta_1| = |\Delta_2| = \pi/2$  for quadruplets 1001 and 0101. As discussed earlier, we have two categories that need to be considered separately.

The first category is when the different symbols belong to constellations with different rotations, for example, quadruplets

1001 and 2011. The CGD depends on the phase difference  $\Delta$  and the difference between the phase of the two symbols. For example, if the different symbols are  $x_1$  and  $x_3$ , the CGD is

$$\text{CGD} = |1 - e^{j\Delta}|^8 |1 - e^{2j(\pi/L + \phi_3 - \phi_1)}|^4. \quad (13)$$

If instead of  $x_1$  and  $x_3$ , the different symbols are  $x_2$  and  $x_4$ , then (13) is still valid after replacing  $\phi_3 - \phi_1$  with  $\phi_4 - \phi_2$ . For QPSK, if  $\Delta = \pi/2$ , for example, quadruplets 2011 and 1001, then  $\text{CGD} = 64$ . On the other hand,  $\Delta = \pi$ , for example, quadruplets 3021 and 1001, results in  $\text{CGD} = 1024$ . Note that  $\phi_3 - \phi_1$  (or  $\phi_4 - \phi_2$ ) is a multiple of  $2\pi/L$  and there are only a few cases that we need to consider for finding the minimum CGD, for example, two cases for BPSK.

The second category is any other pair with two differences. In this case, the two symbols are from constellations with the same rotations, for example, quadruplets 1001 and 0101. The CGD depends on the phase difference  $\Delta$  and can be simplified as follows:

$$\text{CGD} = 16|1 - e^{j\Delta}|^8. \quad (14)$$

For QPSK, if  $\Delta = \pi/2$ , for example quadruplets 0101 and 1001, then  $\text{CGD} = 256$ . On the other hand,  $\Delta = \pi$ , for example, quadruplets 3201 and 1001, results in  $\text{CGD} = 4096$ .

#### C. Three Differences

In this section, we show that we do not need to calculate the CGD in this case (when only one of the symbols is identical between the two quadruplets) in order to calculate the CGD of our set partitioning. The final format of the CGD formula is very similar for different possibilities in this case. Therefore, we only consider the case that the fourth symbols are identical. The resulting CGD is calculated by

$$\text{CGD} = 4|1 - e^{j\Delta}|^8 \left( \left| 1 - \frac{e^{2j(\pi/L + \phi_3 - \phi_1)}}{2} \right|^2 + \frac{9}{4} \right)^2. \quad (15)$$

Since  $4 \left( \left| 1 - \frac{e^{2j(\pi/L + \phi_3 - \phi_1)}}{2} \right|^2 + 9/4 \right)^2 > 1$ , the CGD in (15) is always greater than the one in (12). The structure of our set partitioning is such that the first time that the case of three differences appears it always coincides with the case of only one difference. Therefore, the CGD in (15) is always dominated by the smaller value of (12) and there is no need to calculate it in order to find the minimum CGD.

#### D. Four Differences

Again, due to the structure of our set partitioning, the magnitude of the phase difference between corresponding symbols of

$$\begin{pmatrix} e^{j\phi_1}(1 - e^{j\Delta_1}) & e^{j\phi_2}(1 - e^{j\Delta_2}) & e^{j\phi_3}e^{j\phi}(1 - e^{j\Delta_3}) & e^{j\phi_4}e^{j\phi}(1 - e^{j\Delta_4}) \\ -e^{-j\phi_2}(1 - e^{-j\Delta_2}) & e^{-j\phi_1}(1 - e^{-j\Delta_1}) & -e^{-j\phi_4}e^{-j\phi}(1 - e^{-j\Delta_4}) & e^{-j\phi_3}e^{-j\phi}(1 - e^{-j\Delta_3}) \\ e^{j\phi_3}e^{j\phi}(1 - e^{j\Delta_3}) & e^{j\phi_4}e^{j\phi}(1 - e^{j\Delta_4}) & e^{j\phi_1}(1 - e^{j\Delta_1}) & e^{j\phi_2}(1 - e^{j\Delta_2}) \\ -e^{-j\phi_4}e^{-j\phi}(1 - e^{-j\Delta_4}) & e^{-j\phi_3}e^{-j\phi}(1 - e^{-j\Delta_3}) & -e^{-j\phi_2}(1 - e^{-j\Delta_2}) & e^{-j\phi_1}(1 - e^{-j\Delta_1}) \end{pmatrix} \quad (11)$$

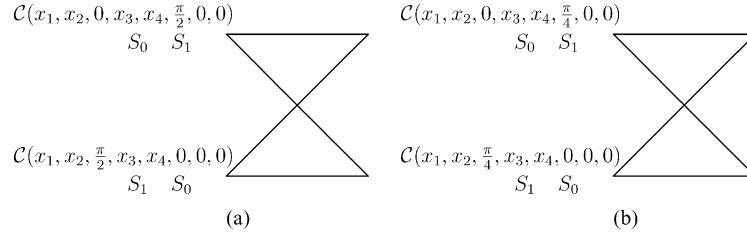


Fig. 4. Two-state codes. (a)  $r = 1$  bit/s/Hz using BPSK. (b)  $r = 2$  bits/s/Hz using QPSK.

the quadruplet is the same. The CGD in this case is calculated as follows:

$$\text{CGD} = 4|1 - e^{j\Delta}|^8 \left( \left| 1 - \frac{e^{2j\phi'_3} + e^{j(\phi'_3 - \phi'_4)} + e^{j(\phi'_3 + \phi'_4)} - 1}{2} \right|^2 + \left| 1 - \frac{e^{2j\phi'_4} + e^{j(\phi'_4 - \phi'_3)} + e^{j(\phi'_3 + \phi'_4)} - 1}{2} \right|^2 \right)^2 \quad (16)$$

where  $\phi'_3 = \pi/L + \phi_3 - \phi_1$  and  $\phi'_4 = \pi/L + \phi_4 - \phi_2$ . For QPSK, if  $\Delta = \pi/2$ , for example quadruplets 2112 and 1001, then  $\text{CGD} = 1024$ . On the other hand,  $\Delta = \pi$ , for example, quadruplets 3223 and 1001, results in  $\text{CGD} = 16384$ .

In this section, we showed how to calculate the CGD in different cases. The derived formulas and the corresponding minimum CGDs match with the direct calculation of CGDs, using the original definition, and a full search to find the minimum CGD. The results are used in the following section to design space-time trellis codes and calculate the coding gain of the designed codes.

## V. DESIGNING FULL-RATE, FULL-DIVERSITY CODES

In this section, we design trellis codes for four transmit antennas and obtain the coding gain for these codes. Using the quasi-orthogonal space-time block codes that we have studied so far as building blocks to design trellis codes would result in rates lower than full rates. To design trellis codes without sacrificing the rate, one should add new elements in the code design as follows. So far, we have assumed that the constellation points  $\tilde{x}_3$  and  $\tilde{x}_4$  belong to a rotated  $L$ -PSK constellation. Obviously, due to the symmetry, similar results are valid if we rotate  $x_1$  and  $x_2$  instead of  $x_3$  and  $x_4$ . This will give us a new degree of freedom and additional constellation matrices to pick from. Using these two codes, we still need more constellation matrices to design full-rate trellis codes. The notion of adding constituent block matrices to the design of an STTC based on phase rotation of one or more columns of the block is analogous to the conversion of an orthogonal code into a super-orthogonal code. Here, we convert a quasi-orthogonal code into a super-quasi-orthogonal code.

Multiplying the  $i$ th column of a quasi-orthogonal code by  $e^{j\theta_i}$  when  $\theta_i$  is a multiple of  $2\pi/L$ , preserves all the characteristics of the code without expanding the constellation. This provides four additional degrees of freedom. In what follows, we show that we only need to use two of these four rotations.

We use  $\mathcal{C}(x_1, x_2, \phi_1, x_3, x_4, \phi_2, \theta_1, \theta_2)$  to represent a quasi-orthogonal code in which symbols are from an  $L$ -PSK con-

stellation; symbols  $x_1$  and  $x_2$  are rotated with rotation  $\phi_1$  and symbols  $x_3$  and  $x_4$  are rotated with rotation  $\phi_2$ . Also, the first column is multiplied by  $e^{j\theta_1}$  and the second column is multiplied by  $e^{j\theta_2}$  as follows:

$$\begin{pmatrix} e^{j\theta_1} e^{j\phi_1} x_1 & e^{j\theta_2} e^{j\phi_1} x_2 & e^{j\phi_2} x_3 & e^{j\phi_2} x_4 \\ -e^{j\theta_1} e^{-j\phi_1} x_2^* & e^{j\theta_2} e^{-j\phi_1} x_1^* & -e^{-j\phi_2} x_4^* & e^{-j\phi_2} x_3^* \\ e^{j\theta_1} e^{j\phi_2} x_3 & e^{j\theta_2} e^{j\phi_2} x_4 & e^{j\phi_1} x_1 & e^{j\phi_1} x_2 \\ -e^{j\theta_1} e^{-j\phi_2} x_4^* & e^{j\theta_2} e^{-j\phi_2} x_3^* & -e^{-j\phi_1} x_2^* & e^{-j\phi_1} x_1^* \end{pmatrix}. \quad (17)$$

Equation (17) provides a class of quasi-orthogonal space-time block codes with four parameters that provide enough constellation matrices to design a full-rate trellis code, when  $x_1, x_2, x_3,$  and  $x_4$  belong to an  $L$ -PSK constellation. There are many other choices that provide similar properties although it is important to make sure that the used rotations do not change the diversity of the code. For example, instead of rotating the first column, one may rotate the third column to achieve a similar code with exactly the same properties. Or as we mentioned before, the codes in (2), (3), and other examples in [7] all provide similar properties after incorporating the proposed rotations. It is easy to show that the above class of codes always provide a full-rate, full-diversity code for which the symbols can be decoded in pairs. Maximum-likelihood decoding for the code in (17) results in finding the pairs  $(x_1, x_3)$  and  $(x_2, x_4)$  separately. The corresponding formulas are provided in the appendix as a reference.

### A. Two-State Codes

We introduce two-state codes for BPSK and QPSK constellations in Fig. 4. It is possible in a two-state code that a path diverging from state zero remerges to state zero in  $P = 2$  transitions. To find the minimum CGD of a code, one should consider all possible paths with  $P = 2$  transitions and calculate the corresponding CGD. Then, the minimum CGD among these paths is compared with the minimum CGD of the parallel paths calculated in Section IV. For the rate  $r = 1$  bit/s/Hz code in Fig. 4 using BPSK, the minimum CGD for paths with  $P = 2$  transitions is more than the minimum CGD for parallel transitions ( $\text{CGD} = 4096$ ). Therefore, the minimum CGD of the code is 4096. For the rate  $r = 2$  bits/s/Hz code in Fig. 4 using QPSK, the minimum CGD of the code is 64 which is dominated by parallel transitions.

Note that one has different choices in selecting the rotations; however, not every possible rotation provides full diversity. For example, in the code presented in Fig. 4(a), picking  $\theta_1 = \pi$  for the first state will result in losing the full diversity. Therefore, it is important to adopt the rotations that preserve the full diversity of the resulting trellis code.

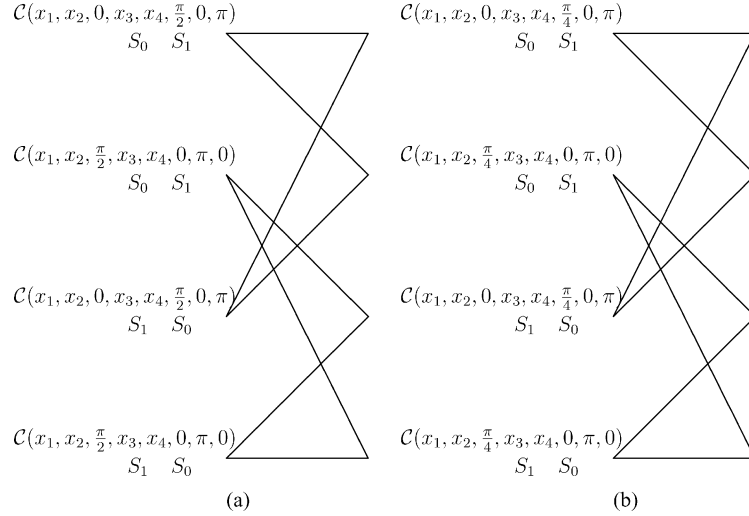


Fig. 5. Four-state codes. (a)  $r = 1$  bit/s/Hz using BPSK. (b)  $r = 2$  bits/s/Hz using QPSK.

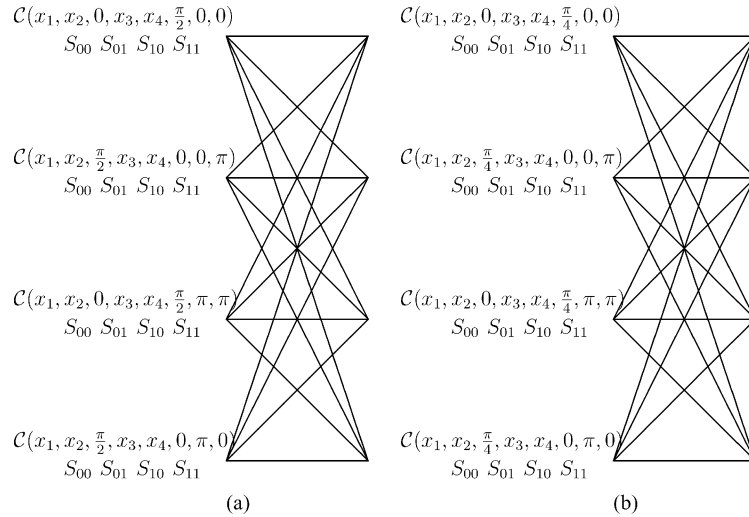


Fig. 6. Four-state codes. (a)  $r = 1$  bit/s/Hz for BPSK. (b)  $r = 2$  bits/s/Hz for QPSK.

### B. Four-State Codes

We demonstrate four-state codes in Fig. 5. It is impossible in these codes to diverge from a state and remerge to the same state after  $P = 2$  transitions. For the BPSK code in Fig. 5, the minimum CGD for the paths with  $P = 3$  transitions is larger than the CGD of parallel transitions which is 4096. Therefore, the minimum CGD of the code is 4096. For the QPSK code in Fig. 5, the minimum CGD of the code is 64 which is also dominated by parallel transitions.

We also present two more four-state codes in Fig. 6. The minimum CGD of the BPSK and QPSK codes in Fig. 6 is 1792 and 256, respectively. The BPSK code in Fig. 6 is more complex than the BPSK code in Fig. 5, while providing a lower coding gain. Therefore, there is no use for this code. On the other hand, the QPSK code in Fig. 6 compared with the QPSK code in Fig. 5 provides a higher coding gain with a slight increase in complexity.

Using our new method, one can design codes for four transmit antennas using any given trellis and at any given rate. Usually,

there are a few degrees of freedom in terms of picking the rotations to maximize the coding gain for the given structure.

### VI. NON-FULL-RATE CODES

In this section, we provide a framework that allows a tradeoff between rate and coding gain. The main idea is to use the structure of a super-orthogonal space-time trellis code designed for two transmit antennas [5] to design space-time trellis codes for four transmit antennas. First, we present the following formula for calculating the CGD of a quasi-orthogonal code from [10]:

$$\text{CGD}_4 = [(\Delta a)^2 - (\Delta b)^2]^2 \quad (18)$$

where

$$\Delta a = \sum_{i=1}^4 |x_i - y_i|^2, \quad \Delta b = \sum_{i=1}^2 2\text{Re}[(x_i - y_i)(x_{2+i} - y_{2+i})^*]. \quad (19)$$

In this section, we use  $\text{CGD}_4$  instead of CGD to emphasize the use of four transmit antennas in the code. We derive a closed-form formula for  $\text{CGD}_4$  in terms of  $\text{CGD}_2$ , the coding gain of

a code for two transmit antennas. For the sake of simplicity, we explain the details for QPSK although a similar approach works for any other  $L$ -PSK constellation.

#### A. QPSK Codes With Rate $r = 1$ bit/s/Hz

First, we design a half-rate code, 1 bit/s/Hz for QPSK, as follows. Four input bits select symbols  $x_1$  and  $x_2$  from the QPSK constellation in a similar way that we pick them in a full-rate code. Then,  $x_3$  and  $x_4$  are assigned as  $x_3 = x_1 e^{j(\pi/4)}$  and  $x_4 = x_2 e^{j(\pi/4)}$ . The following lemma shows how to calculate the coding gain of this code from that of an Alamouti code.

*Lemma 6.1:* For  $x_3 = x_1 e^{j(\pi/4)}$  and  $x_4 = x_2 e^{j(\pi/4)}$ , similar relations for corresponding  $y_i$ , the CGD of a quasi-orthogonal code  $\text{CGD}_4 = 4 \times (\text{CGD}_2)^2$ , where  $\text{CGD}_2$  is the CGD of an Alamouti code using symbols  $x_1$  and  $x_2$ .

*Proof:* Substituting the symbols in (19) results in

$$\Delta a = \sum_{i=1}^2 |x_i - y_i|^2 + \sum_{i=1}^2 |e^{j(\pi/4)}|^2 |x_i - y_i|^2 = 2 \sum_{i=1}^2 |x_i - y_i|^2$$

and

$$\begin{aligned} \Delta b &= \sum_{i=1}^2 2\text{Re} \left[ (x_i - y_i) e^{-j(\pi/4)} (x_i - y_i)^* \right] \\ &= \sum_{i=1}^2 \sqrt{2} |x_i - y_i|^2 = \frac{\Delta a}{\sqrt{2}}. \end{aligned}$$

Therefore, we have  $\text{CGD}_4 = ((\Delta a)^2 - (\Delta b)^2)^2 = (\Delta a)^4/4$ . For the case of two transmit antennas in (1), i.e., the Alamouti code, we have

$$\text{CGD}_2 = \det \left( \begin{pmatrix} |x_1 - y_1|^2 + |x_2 - y_2|^2 & 0 \\ 0 & |x_1 - y_1|^2 + |x_2 - y_2|^2 \end{pmatrix} \right). \quad (20)$$

Defining  $\Delta a_2 = |x_1 - y_1|^2 + |x_2 - y_2|^2$  results in  $\text{CGD}_2 = (\Delta a_2)^2$  and since  $\Delta a_2 = \Delta a/2$ , we have  $\text{CGD}_2 = (\Delta a)^2/4$ , or equivalently

$$\text{CGD}_4 = 4 \times (\text{CGD}_2)^2. \quad (21)$$

□

This provides a remarkable increase in the coding gain by sacrificing half the rate. Note that since  $x_3$  is a function of  $x_1$  and  $x_4$  is a function of  $x_2$ , the maximum-likelihood decoding only needs to provide  $x_1$  and  $x_2$ . Therefore, similar to orthogonal space-time block codes, different symbols are decoded separately and the decoding is very simple. This is unlike the quasi-orthogonal codes for which the decoding is done in pairs using (26) and (27).

The map that we have used to define  $(x_3, x_4)$  from  $(x_1, x_2)$  is not unique. In fact, one can use different possibilities with similar properties in order to increase the rate. We consider such an approach in what follows.

#### B. QPSK Codes With Rate $r = 1.75$ bits/s/Hz

Let us assume that for any constellation pair  $(x_1, x_2)$ , we pick one of the eight possible constellation pairs  $(x_3, x_4)$  from the following list:

$$\begin{aligned} (x_3 &= x_1 e^{j(\pi/4)}, & x_4 &= x_2 e^{j(\pi/4)}) \\ (x_3 &= x_1 e^{j(3\pi/4)}, & x_4 &= x_2 e^{j(3\pi/4)}) \\ (x_3 &= x_1 e^{j(5\pi/4)}, & x_4 &= x_2 e^{j(5\pi/4)}) \\ (x_3 &= x_1 e^{j(7\pi/4)}, & x_4 &= x_2 e^{j(7\pi/4)}) \\ (x_3 &= x_1 e^{j(\pi/4)}, & x_4 &= x_2 e^{j(7\pi/4)}) \\ (x_3 &= x_1 e^{j(7\pi/4)}, & x_4 &= x_2 e^{j(\pi/4)}) \\ (x_3 &= x_1 e^{j(3\pi/4)}, & x_4 &= x_2 e^{j(5\pi/4)}) \\ (x_3 &= x_1 e^{j(5\pi/4)}, & x_4 &= x_2 e^{j(3\pi/4)}). \end{aligned}$$

Then, there are  $16 \times 8 = 2^7$  total possible quadruplets if the constellation is QPSK. Therefore, the rate of the code is  $7/4 = 1.75$  bits/s/Hz.

To calculate the CGD of this code, we use the following parameters to summarize different cases

$$\begin{aligned} x_3 &= x_1 e^{j(\pi/4)m}, & x_4 &= x_2 e^{j(\pi/4)n} \\ (m, n) &\in \{(1, 1)(3, 3), (5, 5), (7, 7) \\ &\quad (1, 7), (7, 1), (3, 5), (5, 3)\}. \end{aligned} \quad (22)$$

*Lemma 6.2:* If  $(x_3, x_4)$  and  $(y_3, y_4)$  are chosen from (22), the CGD of a quasi-orthogonal code  $\text{CGD}_4 = 4 \times (\text{CGD}_2)^2$ , where  $\text{CGD}_2$  is the CGD of an Alamouti code using symbols  $x_1$  and  $x_2$ .

*Proof:* Different terms that are needed in the calculation of CGD are derived as

$$\begin{aligned} |x_3 - y_3|^2 &= |e^{j(\pi/4)m}|^2 |x_1 - y_1|^2 \\ |x_4 - y_4|^2 &= |e^{j(\pi/4)n}|^2 |x_2 - y_2|^2. \end{aligned}$$

As a result,  $\Delta a = 2(|x_1 - y_1|^2 + |x_2 - y_2|^2)^2$ , and similarly

$$\begin{aligned} \Delta b &= 2\text{Re}[(x_1 - y_1)(x_1 - y_1)^* e^{-j(\pi/4)m}] \\ &\quad + 2\text{Re}[(x_2 - y_2)(x_2 - y_2)^* e^{-j(\pi/4)n}] \\ &= 2 \cos\left(\frac{\pi}{4}m\right) |x_1 - y_1|^2 + 2 \cos\left(\frac{\pi}{4}n\right) |x_2 - y_2|^2. \end{aligned} \quad (23)$$

Since  $\cos((\pi/4)m)$  and  $\cos((\pi/4)n)$  are equal for the eight possible cases, we can factor them out resulting in

$$\begin{aligned} (\Delta b)^2 &= \left( 2 \left( \pm \frac{\sqrt{2}}{2} \right) \right)^2 (|x_1 - y_1|^2 + |x_2 - y_2|^2)^2 \\ &= 2 (|x_1 - y_1|^2 + |x_2 - y_2|^2)^2 = \frac{(\Delta a)^2}{2}. \end{aligned} \quad (24)$$

Therefore, CGD is calculated as follows:

$$\text{CGD}_4 = ((\Delta a)^2 - (\Delta b)^2)^2 = \frac{(\Delta a)^4}{4} = 4 \times (\text{CGD}_2)^2 \quad (25)$$

which is identical to (21) and is a high increase in the coding gain. □

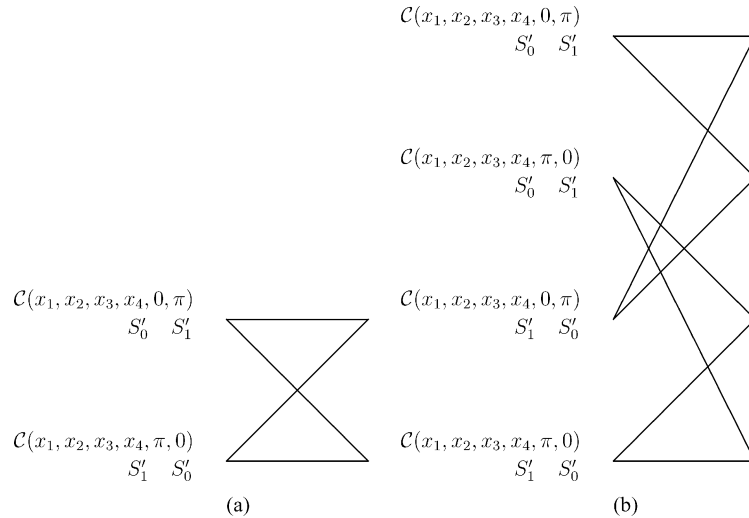


Fig. 7. Non-full-rate codes using QPSK;  $r = 1, 1.5, 1.75$  bits/s/Hz. (a) Two-state codes. (b) Four-state codes.

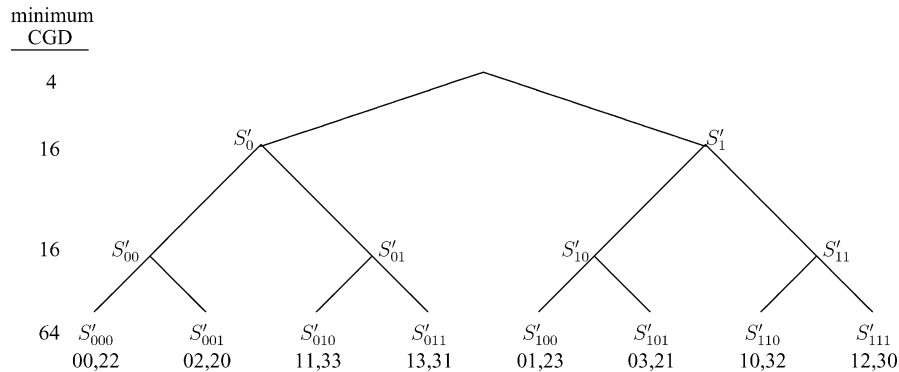


Fig. 8. Set partitioning for QPSK; the numbers at leaves represent the indices of the symbols in the space–time block code for two transmit antennas.

### C. Trellis Diagrams

In this section, we design space–time trellis codes that are not full-rate. Note that using (25), there is a one-to-one mapping between the CGD of our non-full-rate codes and the full-rate super-orthogonal space–time trellis codes for two transmit antennas in [5]. Therefore, we use the optimal set partitioning and codes from [5] and add the above structure to design codes for four transmit antennas. Fig. 7 shows two examples of such codes where with a slight abuse of the notation,  $\mathcal{C}(x_1, x_2, x_3, x_4, \theta_1, \theta_2)$  represents a quasi-orthogonal code in which the first column is multiplied by  $e^{j\theta_1}$  and the second column is multiplied by  $e^{j\theta_2}$ . The set partitioning for  $(x_1, x_2)$  is the same as the set partitioning in [5] for a space–time block code using orthogonal designs and two transmit antennas and is shown in Fig. 8. Symbols  $x_3$  and  $x_4$  are selected as we discussed in Sections VI-A and VI-B. For the codes with rate  $r = 1.75$  bits/s/Hz, each trellis transition represents eight different possibilities for  $(x_3, x_4)$  from (22). By using four of the eight cases in (22), one can design a rate  $r = 1.5$  bits/s/Hz code using the same trellis. It can be shown that after multiplying the  $i$ th column by  $e^{j\theta_i}$ , the CGD is still calculated by (25). Also, for a path with  $P$  transitions, the CGD is calculated by replacing the  $\Delta a$  in (25) with the sum of the corresponding  $\Delta a$ 's for each transition, i.e.,  $\Delta a = \sum_{p=1}^P (\Delta a)_p$ . Considering a super-orthogonal space–time trellis code for two transmit

antennas and a path with  $P$  transitions  $\text{CGD}_2 = (\Delta a)^2/4$ , where  $\Delta a$  is the same as before, i.e.,  $\Delta a = \sum_{p=1}^P (\Delta a)_p$ . Therefore, (25) holds for any path with  $P$  transitions. Since the set partitioning is taken from [5], and we have (25) for the CGD, all optimality results from [5] hold in this case as well. Since the minimum CGD of the two-state and four-state super-orthogonal space–time codes for two transmit antennas is 16 [5], using (25), the minimum CGD of the codes in Fig. 7 is 1024. This is much more than 64, the minimum CGD of the QPSK code in Fig. 5, although the rate of the QPSK code in Fig. 5 is 2 bits/s/Hz. Note that in general a higher CGD is expected for a lower rate code. Therefore, there is a tradeoff between rate and coding gain using non-full-rate codes versus full-rate codes.

Given any super-orthogonal space–time trellis code designed for two transmit antennas in [5], the structure in this section allows us to design space–time trellis codes for four transmit antennas and therefore provides a tradeoff between rate and coding gain.

## VII. SIMULATION RESULTS

In this section, we provide the simulation results of the codes that we designed in Sections V and VI for four transmit antennas and one receive antenna. In all simulations, a frame consists of 132 transmissions out of each transmit antenna. We consider

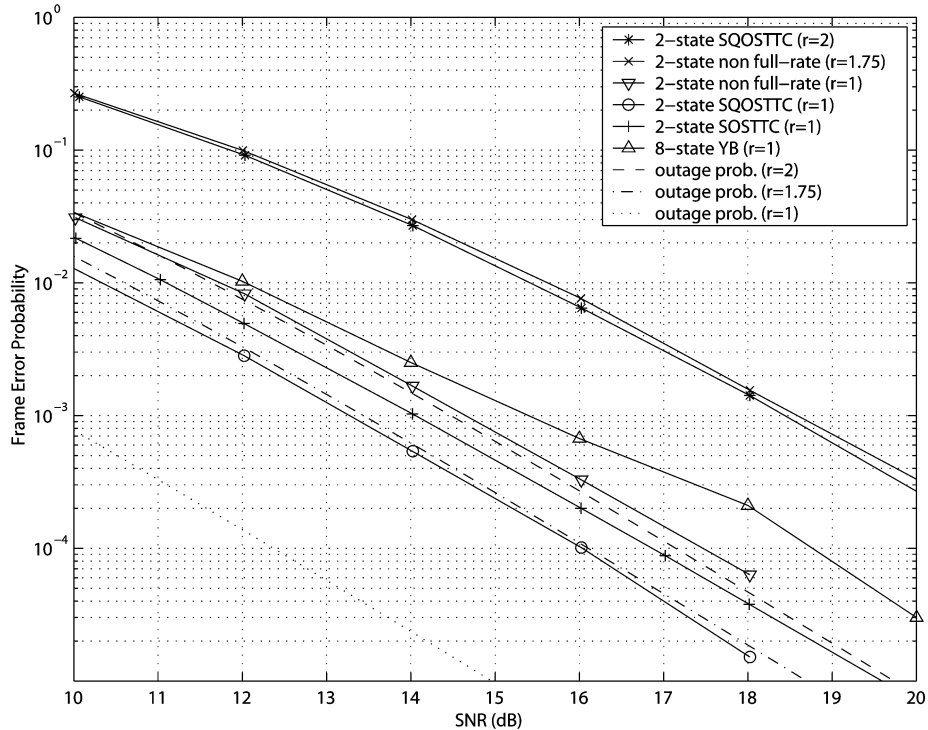


Fig. 9. Simulation results for four transmit antennas and one receive antenna.

a quasi-static Rayleigh-fading channel in which the fades are constant over a frame and change independently for each frame. Fig. 9 shows the frame error probability results versus SNR for different codes. The two-state codes in Fig. 4 are denoted by SQOSTTC ( $r = 1$ ) and SQOSTTC ( $r = 2$ ). The set partitioning in Fig. 1 is used for BPSK ( $r = 1$  bit/s/Hz). For  $r = 2$  bits/s/Hz, we use QPSK and the corresponding set partitioning in Table I. We also include the non-full-rate codes in Section VI for  $r = 1$ , 1.75 bits/s/Hz. While the CGD of these two codes are the same and equal to 1024, the non-full-rate  $r = 1$  code may not be a good candidate because a higher CGD is possible using BPSK in a SOSTTC or SQOSTTC structure. On the other hand, the  $r = 1.75$  code is a very good candidate. Note that in general the CGD is higher for a lower rate code and there is a tradeoff between coding gain and the rate of a code. At rate  $r = 1$  bit/s/Hz, we provide two other codes for comparison. The second code is an eight-state space-time code from [17]. In addition, we include outage probabilities from [18] (independently derived in [19]). The results show that the slope of the curve for SQOSTTCs is the same as that of the outage probability. This is in agreement with the fact that SQOSTTCs provide full diversity. Also, using only two states, the performance of SQOSTTCs is about 3.5–4 dB away from the outage capacity. The gap can be decreased by using a trellis with more states.

As can be seen from the simulation results, the rate  $r = 2$  bits/s/Hz full-rate code and the rate  $r = 1.75$  bits/s/Hz non-full-rate code using four transmit antennas provide all good properties of SOSTTCs using two transmit antennas. Therefore, one can think of SQOSTTCs as generalization of SOSTTCs to more than two transmit antennas. As can be seen from the figure, our two-state SQOSTTC outperforms an eight-state code from [17] at high SNRs, while providing

TABLE II  
CGD ( $x$  CAN BE 0 OR 1)

Subset	QPSK	BPSK
	CGD	CGD
$S$	16	256
$S_x$	64	4096
$S_{xx}$	256	4096
$S_{xxx}$	256	65536
$S_{xxxx}$	1024	
$S_{xxxxx}$	1024	
$S_{xxxxxx}$	4096	
$S_{xxxxxxx}$	16384	

a lower complexity. It also outperforms a two-state SOSTTC. Since the gap between SQOSTTCs and outage probabilities is similar at rates  $r = 1, 2$ , we expect a similar comparison and the superiority of SQOSTTCs at  $r = 2$  bits/s/Hz although it is not shown in the figure due to the lack of access to the simulation results of other codes.

## VIII. CONCLUSION

In this paper, we have presented and analyzed new codes named *super-quasi-orthogonal space-time trellis codes* for four transmit antennas. First, we provided the necessary and sufficient condition for full diversity in quasi-orthogonal codes. Then, we used these results to present full-diversity, full-rate super-quasi-orthogonal codes. These codes combine set partitioning and a super set of quasi-orthogonal space-time block codes in a systematic way to provide full diversity and improved

coding gain. The result is a powerful code that provides full rate, full diversity, and high coding gain for different number of states and at different rates. Then, we introduced non-full-rate codes that provide higher coding gains compare with full-rate codes. It is also possible to maintain a tradeoff between coding gain and rate. Simulation results demonstrate the good performance of our new super-quasi-orthogonal space–time trellis codes. We have provided a complete study of CGD analysis and different code examples. There are few examples of codes for more than two transmit antennas in the literature. The existing space–time codes in the literature are usually designed manually or by computer search, while our proposed codes are designed systematically. Also, simulation results show that our codes provide very good performance with only two states.

In this paper, we only consider four transmit antennas. quasi-orthogonal space–time block codes have been designed for more than four transmit antennas as well [7], [8]. Our proposed space–time trellis codes are general enough such that one can design codes for more than four transmit antennas following similar methods. The details and performance results can be considered as future work.

#### APPENDIX

In this Appendix, we provide the decoding formulas for the quasi-orthogonal space–time block code in (17) and one receive antenna. Maximum-likelihood decoding for the code in (17) results in finding the pair  $(x_1, x_3)$  that minimizes  $f_{13}(x_1, x_3)$  in the following equation:

$$\begin{aligned} f_{13}(x_1, x_3) &= \left( \sum_{n=1}^4 |\alpha_n|^2 \right) (|x_1 e^{j\phi_1}|^2 + |x_3 e^{j\phi_2}|^2) \\ &\quad - 2\text{Re} \left[ x_1 e^{j\phi_1} (r_1^* \alpha_1 e^{j\theta_1} + r_2^* \alpha_2 e^{-j\theta_2} + r_3^* \alpha_3 + r_4^* \alpha_4^*) \right. \\ &\quad \left. + x_3 e^{j\phi_2} (r_1^* \alpha_3 + r_2^* \alpha_4^* + r_3^* \alpha_1 e^{j\theta_1} + r_4^* \alpha_2^* e^{-j\theta_2}) \right] \\ &\quad + 4\text{Re} \left[ x_1 x_3^* e^{j(\phi_1 - \phi_2)} \right] \text{Re} \left[ \alpha_1 \alpha_3^* e^{j\theta_1} + \alpha_2 \alpha_4^* e^{j\theta_2} \right]. \end{aligned} \quad (26)$$

where  $\alpha_n$ ,  $n = 1, 2, 3, 4$  is the path gain from the  $n^{\text{th}}$  transmit antenna to the receive antenna and  $r_t$ ,  $t = 1, 2, 3, 4$  is the received signal at time  $t$ . Note that if  $\text{Re} [x_1 x_3^* e^{j(\phi_1 - \phi_2)}] = 0$ , there is no cross term and independent decoding of  $x_1$  and  $x_3$  is possible. One such an example is when  $x_1$  and  $x_3$  are real numbers, while  $\phi_1 = 0$  and  $\phi_2 = \pi/2$ . Similarly, maximum-likelihood decoding results in finding the pair  $(x_2, x_4)$  that minimizes  $f_{24}(x_2, x_4)$  in the following equation:

$$\begin{aligned} f_{24}(x_2, x_4) &= \left( \sum_{n=1}^4 |\alpha_n|^2 \right) (|x_2 e^{j\phi_1}|^2 + |x_4 e^{j\phi_2}|^2) \\ &\quad - 2\text{Re} \left[ x_2 e^{j\phi_1} (r_1^* \alpha_2 e^{j\theta_2} - r_2^* \alpha_1^* e^{-j\theta_1} + r_3^* \alpha_4 - r_4^* \alpha_3^*) \right. \\ &\quad \left. + x_4 e^{j\phi_2} (r_1^* \alpha_4 - r_2^* \alpha_3^* + r_3^* \alpha_2 e^{j\theta_2} - r_4^* \alpha_1^* e^{-j\theta_1}) \right] \\ &\quad + 4\text{Re} \left[ x_2 x_4^* e^{j(\phi_1 - \phi_2)} \right] \text{Re} \left[ \alpha_1 \alpha_3^* e^{j\theta_1} + \alpha_2 \alpha_4^* e^{j\theta_2} \right]. \end{aligned} \quad (27)$$

Again,  $x_2$  and  $x_4$  can be decoded independently if  $\text{Re} [x_2 x_4^* e^{j(\phi_1 - \phi_2)}] = 0$ . In general, the pairs  $(x_1, x_3)$  and  $(x_2, x_4)$  are decoded separately. If  $\text{Re} [x_1 x_3^* e^{j(\phi_1 - \phi_2)}] = \text{Re} [x_2 x_4^* e^{j(\phi_1 - \phi_2)}] = 0$ , all symbols can be decoded independently and the resulting code is a pseudo-orthogonal space–time block code [20].

#### ACKNOWLEDGMENT

The authors would like to thank Dr. Q. Yan for providing the simulation results of a space–time code in [17].

#### REFERENCES

- [1] V. Tarokh, N. Seshadri, and A. R. Calderbank, "Space–time codes for high data rate wireless communication: Performance analysis and code construction," *IEEE Trans. Inf. Theory*, vol. 44, no. 2, pp. 744–765, Mar. 1998.
- [2] S. M. Alamouti, "A simple transmitter diversity scheme for wireless communications," *IEEE J. Sel. Areas Commun.*, vol. 16, no. 8, pp. 1451–1458, Oct. 1998.
- [3] V. Tarokh, H. Jafarkhani, and A. R. Calderbank, "Space–time block codes from orthogonal designs," *IEEE Trans. Inf. Theory*, vol. 45, no. 5, pp. 1456–1467, Jul. 1999.
- [4] —, "Space–time block coding for wireless communications: Performance results," *IEEE J. Sel. Areas Commun.*, vol. 17, no. 3, pp. 451–460, Mar. 1999.
- [5] H. Jafarkhani and N. Seshadri, "Super-orthogonal space–time trellis codes," *IEEE Trans. Inf. Theory*, vol. 49, no. 4, pp. 937–950, Apr. 2003.
- [6] S. Siwamogsatham and M. P. Fitz, "Improved high rate space–time codes via orthogonality and set partitioning," in *Proc. IEEE Wireless Commun. Netw. Conf.*, Mar. 2002, pp. 264–270.
- [7] H. Jafarkhani, "A quasi-orthogonal space–time block code," *IEEE Trans. Commun.*, vol. 49, no. 1, pp. 1–4, Jan. 2001.
- [8] O. Tirkkonen, A. Boariu, and A. Hottinen, "Minimal nonorthogonality rate 1 space–time block code for 3+ Tx antennas," in *Proc. IEEE 6th Int. Symp. Spread-Spectrum Tech. Appl.*, Sep. 2000, pp. 429–432.
- [9] O. Tirkkonen, "Optimizing space–time block codes by constellation rotations," in *Proc. Finnish Wireless Commun. Workshop*, Oct. 2001.
- [10] W. Su and X. Xia, "Signal constellations for quasi-orthogonal space–time block codes with full diversity," *IEEE Trans. Inf. Theory*, vol. 50, no. 10, pp. 2331–2347, Oct. 2004.
- [11] N. Sharma and C. B. Papadias, "Improved quasi-orthogonal codes through constellation rotation," *IEEE Trans. Commun.*, vol. 51, no. 3, pp. 332–335, Mar. 2003.
- [12] V. M. DaSilva and E. S. Sousa, "Fading-resistant modulation using several transmitter antennas," *IEEE Trans. Commun.*, vol. 45, no. 10, pp. 1236–1244, Oct. 1997.
- [13] M. O. Damen, K. Abed-Meraim, and J. C. Belfiore, "Diagonal algebraic space–time block codes," *IEEE Trans. Inf. Theory*, vol. 48, no. 3, pp. 628–636, Mar. 2002.
- [14] Y. Xin, Z. Wang, and G. B. Giannakis, "Space–time diversity systems based on linear constellation precoding," *IEEE Trans. Wireless Commun.*, vol. 2, no. 2, pp. 294–309, Mar. 2003.
- [15] D. Divsalar and M. K. Simon, "Multiple trellis coded modulation (MTCM)," *IEEE Trans. Commun.*, vol. 36, no. 4, pp. 410–419, Apr. 1988.
- [16] P. A. Baker, "Phase-modulation data sets for serial transmission at 2000 and 2400 bits per second, Part I," *AIEE Trans. Commun. Electron.*, Jul. 1962.
- [17] Q. Yan and R. S. Blum, "Improved space–time convolutional codes for quasi-static fading channels," *IEEE Trans. Wireless Commun.*, vol. 1, no. 4, pp. 563–571, Oct. 2002.
- [18] G. J. Foschini and M. Gans, "On the limits of wireless communication in a fading environment when using multiple antennas," *Wireless Pers. Commun.*, vol. 6, pp. 311–335, Mar. 1998.
- [19] E. Teletar, "Capacity of multi-antenna Gaussian channels," *Eur. Trans. Telecommun.*, vol. 10, pp. 585–595, Nov./Dec. 1999.
- [20] H. Jafarkhani and F. Taherkhani, "Pseudo orthogonal designs as space–time block codes," in *Proc. IEEE Int. Symp. Advances Wireless Commun.*, Sep. 2002, pp. 79–80.



**Hamid Jafarkhani** received the B.S. degree in electronics from Tehran University, Tehran, Iran, in 1989 and the M.S. and Ph.D. degrees in electrical engineering from the University of Maryland, College Park, in 1994 and 1997, respectively.

From June 1996 to September 1996, he was a Summer Intern at Lucent Technologies (Bell Laboratories). He joined AT&T Laboratories-Research as a Senior Technical Staff Member in 1997. Later, he was promoted to a Principle Technical Staff Member. He was with Broadcom Corporation, as a Senior

Staff Scientist from 2000 to 2001. Currently, he is an Associate Professor in the Department of Electrical Engineering and Computer Science, University of California, Irvine, where he is also the Deputy Director of the Center for Pervasive Communications and Computing.

Dr. Jafarkhani ranked first in the nationwide entrance examination of Iranian universities in 1984. He was a corecipient of the American Division Award of the 1995 Texas Instruments DSP Solutions Challenge. He received the Best Paper Award of ISWC in 2002 and the National Science Foundation (NSF) Career Award. He is an Associate Editor for the *IEEE COMMUNICATIONS LETTERS* and the *IEEE TRANSACTIONS ON WIRELESS COMMUNICATIONS*.



**Navid Hassanpour** was born in Tehran, Iran, on September 11, 1980. He received the B.S. degree in electrical engineering and the M.S. degree in communication systems from Sharif University of Technology, Tehran, Iran, in 2001 and 2002, respectively, and the M.S. degree in electrical engineering from Stanford University, Stanford, CA, in 2004. He is currently working towards the Ph.D. degree in electrical engineering at Stanford University.

His research interests include coding and information theory for wireless communications and their applications to multiuser, multiple antenna systems.